1. J.W. Watson, P.J. Pella, B.D. Anderson, A.R. Baldwin, T. Chittrakarn, B.S. Flanders, R. Madey, C.C. Foster, and I.J. van Heerden, Phys. Lett. B **181**, 47 (1986).
2. J.W. Watson, B.D. Anderson, and R. Madey, Can. J. Phys. **65**, 566 (1987).
3. W.-M. Zhang, *et al.*, Phys. Rev. C **45**, 2819 (1992).
4. J.W. Watson, B.D. Anderson, A.R. Baldwin, C.C. Foster, D.L. Lamm, R. Madey, P.J. Pella, Y. Wang, and W.-M. Zhang, Nucl. Phys. **A577**, 79c (1994).
5. J.W. Watson, Marco R. Plumley, P.J. Pella, B.D. Anderson, A.R. Baldwin, and R. Madey, Nucl. Instrum. & Methods **A272**, 750 (1988).
6. R. Madey, *et al.*, Nucl. Instrum. & Methods **A214**, 401 (1983).
7. T.N. Taddeucci, *et al.*, Phys. Rev. Lett. **52**, 1960 (1984).

CALIBRATION OF A NEUTRON POLARIMETER

I. Niculescu, R. Madey, T. Eden, K. Baker, and G. Niculescu
Hampton University, Hampton, Virginia, 23668

B.D. Anderson, A.R. Baldwin, M. Elaasar, D. Keane,
A. Lai, H. Liu, R. Madey, D.M. Manley, M. Niboh, M. Olson,
R. Suleiman, J.W. Watson, W.-M. Zhang, and J. Anderson
Kent State University, Kent, Ohio, 44242

J. Cameron, E.J. Stephenson, and C.C. Foster
Indiana University Cyclotron Facility, Bloomington, Indiana, 47408

C.C. Chang, J.J. Kelly, P. Markowitz, C. Halli, and W.R. Brown
University of Maryland, College Park, Maryland, 20742

C. Howell and R. Walter
Duke University, Durham, North Carolina, 27708

We measured the average analyzing power and the efficiency of a neutron polarimeter that was designed for use in experiments to measure the electric form factor of the neutron at the Bates Linear Accelerator Center and at the Continuous Electron Beam Accelerator Facility. The experiment was performed with polarized protons at the Indiana University Cyclotron Facility. The detector station that housed the polarimeter was located outside of the beam-swinger facility on the zero-degree line at a flight path of 65.55 m from the target to the midpoint of the front analyzing detector array in the polarimeter.

Shown in Fig. 1 is the configuration of the neutron polarimeter that was calibrated. A description of this polarimeter was reported previously.[1] It consists of 20 plastic (NE102) scintillation detectors: eight front scattering analyzers and two rear arrays parallel to the central ray of the incident neutron flux. Each rear array consists of two layers of detectors; each layer is composed of three detectors stacked side by side and staggered. Each detector

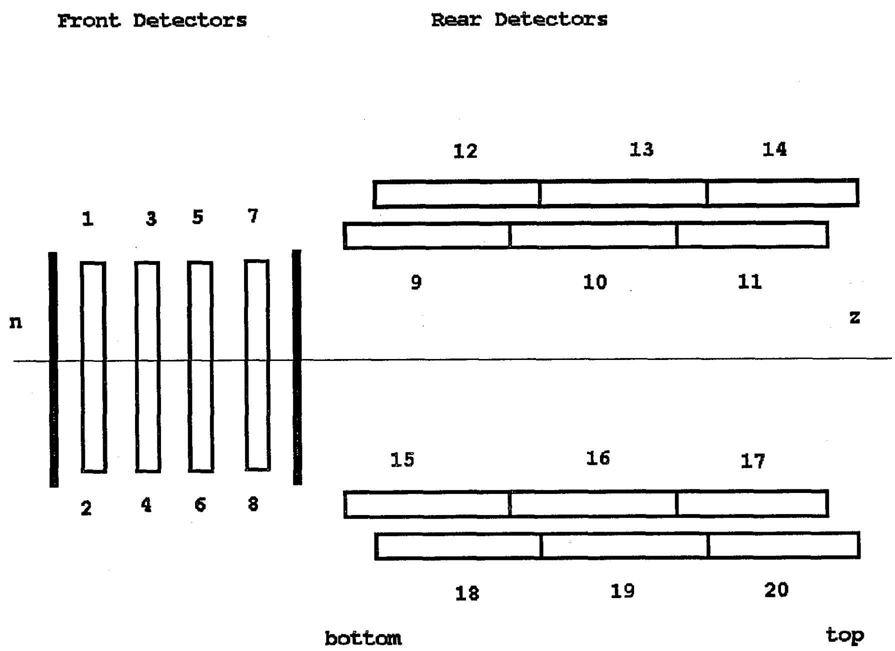

Figure 1. Configuration of the neutron polarimeter used in this experiment.

is 101.8 cm long × 50.8 cm wide × 10.16 cm thick. The eight front scintillators are 101.6 cm long × 25.4 cm high × 10.16 cm thick. Placed immediately at the front and rear of the front detector array are thin (0.95 cm) plastic counters to veto charged particles. The design of the polarimeter is based on the properties of n–p scattering as a polarization analyzer.

In order to simulate the experimental conditions at Bates, a lead-steel wall was constructed. The purpose of this wall is to shield the neutron polarimeter from the charged particles and high energy photons coming from the target. The wall consisted of 4″ of lead sandwiched between two layers of 1.38-in thick steel. This wall was located about 25″ in front of the polarimeter. The wall was supported on concrete blocks.

The principle of measuring the average analyzing power and the efficiency for an earlier neutron polarimeter was described previously.[2] The average analyzing power $\langle A_y \rangle$ of the polarimeter can be obtained by measuring the average scattering asymmetry $\langle \xi \rangle$ for neutrons of known polarization. To obtain a neutron flux of known polarization, we used the $0^+ \rightarrow 0^+$ transition to the isobaric analog state in the $^{14}C(\vec{p},\vec{n})^{14}N$ (2.31 MeV) reaction at 0°. The polarization of the incident proton beam (which for this state is equal to the polarization of the neutron) was 74.5%±0.5% for this experiment. The double-scattering efficiency of the polarimeter was measured by making use of the 0° cross sections of Anderson, *et al.*,[3] for the $^{12}C(p,n)^{12}N$(g.s.) reaction (which has a Q-value of –18.1 MeV) and those of Taddeucci, *et al.*, for the $^{14}C(p,n)^{14}N(3.95\ \mathrm{MeV}, 1^+)$ reaction (which has a Q-value of –4.58 MeV).[4]

The calibration was done at three different neutron energies: 195, 159.5 and 120 MeV. The incident proton energy was selected such as to obtain these neutron energies. At 159.5 MeV, we measured the analyzing power and efficiency with and without the lead-steel wall. Here we report only the results for $T_n = 159.5$ MeV.

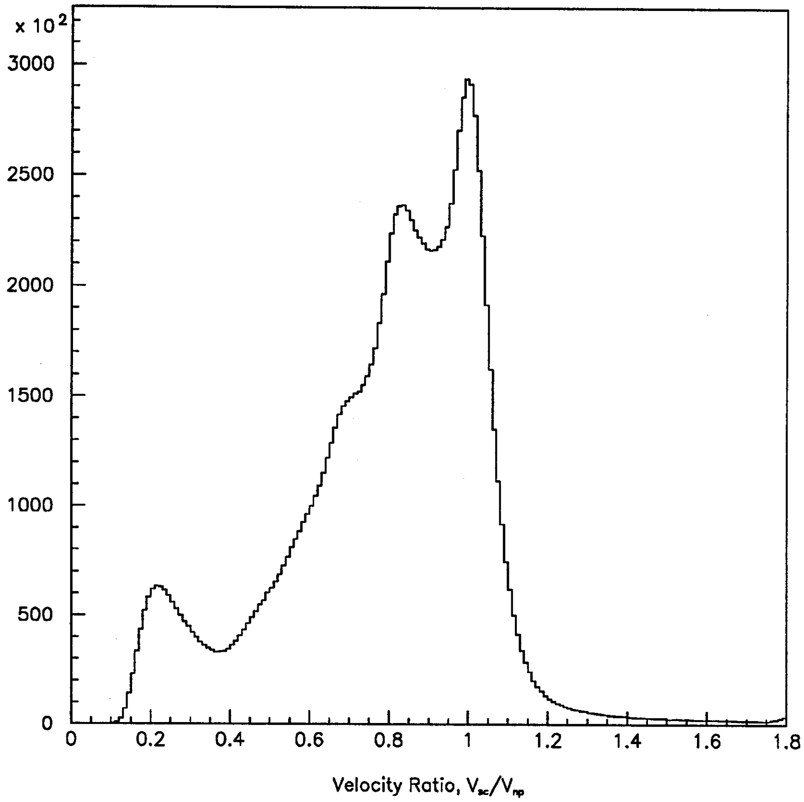

Figure 2. Spectrum of the velocity ratio $R_v = v_{sc}/v_{np}$ for a neutron kinetic energy of 159.5 MeV.

The analysis was done using two different methods. The first method was described in an earlier paper.[2] For this method, the measured velocity of the scattered neutron v_{sc} was determined from the calculated flight path and the time-of-flight between the front scatterer and a rear detector. This scattered velocity was compared with the velocity calculated for n–p scattering v_{np}. The kinetic energy of the scattered neutron T_{np} is given by:

$$T_{np} = \frac{2T_{inc}\cos^2\theta}{(\gamma+1)-(\gamma-1)\cos^2\theta}.$$

Events were rejected if v_{sc} was not sufficiently close to v_{np}. The cut on the velocity ratio ($R_v = v_{sc}/v_{np}$) is needed to discriminate against background events from the C(n,np) reaction on carbon nuclei in the scatterer. A typical spectrum of the velocity ratio is shown in Fig. 2 for $T_n = 159.5$ MeV. Results for this method are shown in Tables I A and I B for an incident neutron energy of 159.5 MeV.

In the second method, the events from the C(n,np) reaction were rejected by selecting a portion of the time-of-flight spectra from one of the front analyzers to one of the rear detectors. Shown in Fig. 3 is a typical rear-to-front time-of-flight spectrum (from front

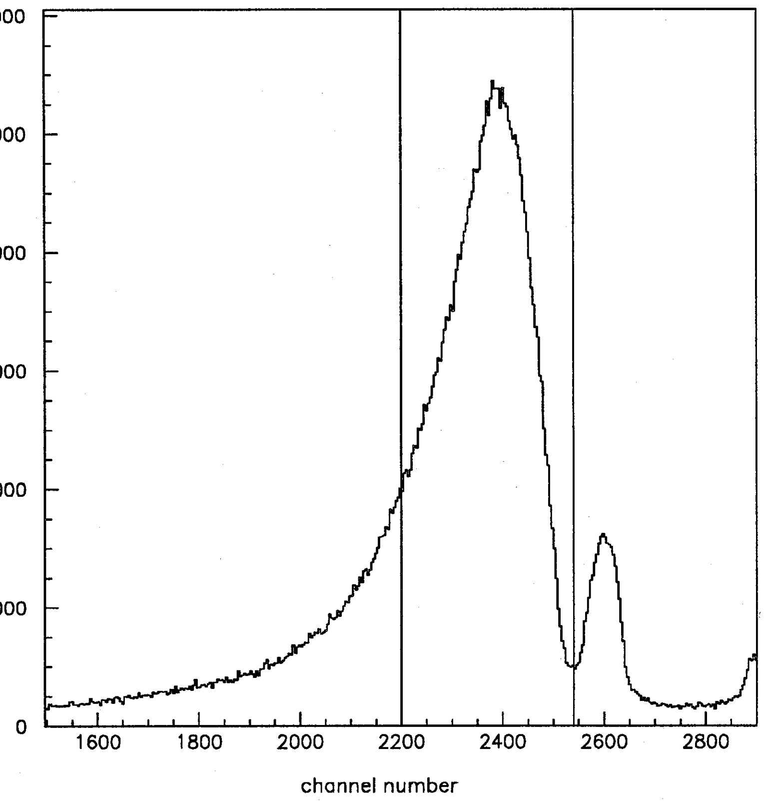

Figure 3. Typical time-of-flight spectrum from front detector 6 to rear detector 9 with hardware thresholds only. The analysis was done using software pulse-height thresholds of 4 MeV-ee for the front detectors and 10 MeV-ee for the rear detectors.

detector 6 to rear detector 9). This spectrum has a gradual rise (for longer times) and a sharp falloff (predominantly from the edge of elastic n–p scattering). After this broad peak, there is a γ-peak. In order to separate the n–p events, we applied an upper cut just at the left of this γ-peak; the lower cut is determined so that only a certain percent of the events are retained. The region between the two vertical lines in Fig. 3 contains the events analyzed. The asymmetry, the analyzing power, the efficiency, and the figure of merit and their relative uncertainties are listed in Tables II A and II B as a function of the fraction of events analyzed.

For both methods we observe that the asymmetry and the analyzing power increase and the efficiency decreases, as we reject more events. The figure of merit has a maximum at about $R_V = 0.93$ for the velocity ratio method of analysis; for the second method of analysis, the maximum corresponds to about 45% of events being retained.

The analyzing powers obtained from the run with the Pb-Fe wall are slightly smaller than the ones obtained without the wall. As discussed previously,[2] there may be a small neutron depolarization in the lead-steel wall. A preliminary calculation[5] based on a simplified geometry for 160-MeV neutrons finds factors of 0.984 for Pb and 0.982 for Fe for a net

Table I A. Asymmetry $\langle\xi\rangle$, analyzing power $\langle A_y\rangle$, efficiency ϵ, and figure of merit $\eta[\equiv \langle A_y\rangle^2\epsilon]$ as a function of the velocity ratio $R_v[= v_{sc}/v_{np}]$ for 159.5-MeV neutrons incident on the neutron polarimeter with a Pb-Fe wall. These data are based on events between R_v and $R_v^{max} = 1.4$.

R_v	$\langle\xi\rangle$	$\langle A_y\rangle$	ϵ (%)	η (%)	events retained (%)
0.00	0.108±0.005	0.145±0.006	0.40	0.0084	100
0.30	0.110±0.005	0.148±0.006	0.39	0.0086	91
0.50	0.115±0.005	0.154±0.006	0.38	0.0090	82
0.60	0.122±0.005	0.163±0.006	0.36	0.0095	74
0.70	0.136±0.005	0.183±0.006	0.32	0.011	62
0.80	0.158±0.005	0.213±0.007	0.26	0.012	49
0.90	0.202±0.005	0.271±0.007	0.19	0.014	31
0.93	0.223±0.006	0.299±0.008	0.16	0.014	28
0.94	0.229±0.006	0.307±0.008	0.15	0.014	26
0.95	0.235±0.006	0.316±0.008	0.14	0.014	25
0.97	0.244±0.006	0.329±0.009	0.12	0.013	21

depolarization of 3.4%. These results may depend slightly on the optical model. A Monte Carlo simulation would be needed to treat the geometrical configuration properly. The difference obtained experimentally for this polarimeter is consistent with this value. The efficiency is the same with and without the Pb-Fe wall because the efficiency depends only on neutrons incident on the first detector of the polarimeter. The statistical uncertainties for the analyzing power are smaller than the ones obtained in an earlier calibration run[2] with a V–shaped polarimeter used for Bates E85-05. For runs without the wall, the statistical uncertainties $\Delta\langle A_y\rangle/\langle A_y\rangle$ are typically 2% here, compared to 3.2% for the calibration of the old polarimeter.

1. R. Madey, *et al.*, Bull. Am. Phys. Soc. **39**, 1055 (1994); R. Madey, *et al.*, *Proc. of the 8th Int. Symp. on Polarization Phenomena in Nucl. Phys.* (AIP, 1994) (in press).
2. T. Eden, *et al.*, Nucl. Instrum. & Methods **A338**, 432 (1994).
3. B.D. Anderson, *et al.*, Phys. Rev. C **26**, 8 (1982).
4. T.N. Taddeucci, *et al.*, Nucl. Phys. **A469**, 125 (1987).
5. J.J. Kelly (unpublished).

Table I B. Asymmetry $\langle \xi \rangle$, analyzing power $\langle A_y \rangle$, efficiency ϵ, and figure of merit $\eta[\equiv \langle A_y \rangle^2 \epsilon]$ as a function of the velocity ratio $R_v[= v_{sc}/v_{np}]$ for 159.5-MeV neutrons incident on the neutron polarimeter without a Pb-Fe wall. These data are based on events between R_v and $R_v^{max} = 1.4$.

R_v	$\langle \xi \rangle$	$\langle A_y \rangle$	ϵ (%)	η (%)	events retained (%)
0.00	0.114±0.003	0.153±0.004	0.43	0.010	100
0.30	0.117±0.003	0.157±0.004	0.42	0.010	94
0.50	0.123±0.003	0.165±0.004	0.40	0.011	87
0.60	0.131±0.003	0.175±0.004	0.38	0.012	81
0.70	0.145±0.003	0.194±0.005	0.34	0.012	70
0.80	0.168±0.003	0.225±0.005	0.29	0.015	57
0.90	0.211±0.004	0.282±0.005	0.21	0.017	38
0.93	0.231±0.004	0.310±0.005	0.18	0.017	35
0.94	0.237±0.004	0.318±0.006	0.17	0.017	33
0.95	0.246±0.004	0.329±0.006	0.16	0.018	29
0.97	0.257±0.004	0.344±0.006	0.14	0.016	27

Table II A. Asymmetry $\langle\xi\rangle$, analyzing power $\langle A_y\rangle$, efficiency ϵ, and figure of merit $\eta[\equiv \langle A_y\rangle^2\epsilon]$ as a function of the percent of events retained in the ΔTOF spectrum for 159.5-MeV neutrons incident on the neutron polarimeter with a Pb-Fe wall.

% events retained	$\langle\xi\rangle$	$\langle A_y\rangle$	ϵ (%)	η (%)
100	0.111±0.005	0.149±0.007	0.39	0.0086
80	0.122±0.005	0.164±0.007	0.35	0.0093
55	0.150±0.005	0.202±0.007	0.28	0.011
50	0.159±0.005	0.214±0.007	0.25	0.011
45	0.165±0.005	0.222±0.007	0.24	0.012
40	0.173±0.005	0.232±0.007	0.22	0.012
30	0.186±0.006	0.250±0.008	0.17	0.010
20	0.209±0.007	0.281±0.010	0.12	0.0090
10	0.246±0.009	0.331±0.013	0.06	0.0066

Table II B. Asymmetry $\langle\xi\rangle$, analyzing power $\langle A_y\rangle$, efficiency ϵ, and figure of merit $\eta[\equiv \langle A_y\rangle^2\epsilon]$ as a function of the percent of events retained in the ΔTOF spectrum for 159.5-MeV neutrons incident on the neutron polarimeter without a Pb-Fe wall.

% events retained	$\langle\xi\rangle$	$\langle A_y\rangle$	ϵ (%)	η (%)
100	0.115±0.003	0.154±0.005	0.42	0.0099
80	0.132±0.003	0.176±0.005	0.36	0.011
55	0.168±0.004	0.225±0.005	0.27	0.014
50	0.174±0.004	0.233±0.005	0.25	0.014
45	0.188±0.004	0.252±0.005	0.23	0.015
40	0.189±0.004	0.252±0.006	0.21	0.013
30	0.207±0.004	0.277±0.006	0.16	0.012
20	0.227±0.005	0.303±0.007	0.11	0.010
10	0.261±0.007	0.349±0.010	0.06	0.0068